

Ruoxi Wang^{1*}

Comic Image Segmentation and Adaptive Differential Evolution Algorithm with Different Times Characteristics: Based on Deep Playv

3+



Abstract: - Comic image segmentation involves dividing a comic image into distinct regions representing various elements like characters, backgrounds, and speech balloons to aid analysis, comprehension, and manipulation for tasks such as content retrieval, archiving, and production. However, accurately discerning between diverse visual elements, particularly in intricate or stylized artwork, poses a significant challenge. This manuscript proposes Comic Image Segmentation and Adaptive DE Algorithm with Different Times Characteristics (CIS-DTC-ADEA). Initially, the pictures collected from Comic Art information set are provided as input. The pictures are then sent into pre-processing. In pre-processing, Fast Resampled Iterative Filtering (FRIF) is used for noise removal, blur, and binary thresholding. After pre-process the output is fed to Deep Attention Dilated Residual DADRCNN for the classification of image. In general real and Synthetic Images was given for classification ADEA to optimize the Deep DADRCNN for classifying images us manga and classic. The proposed CIS-DTS-ADEA approach is applied in python working platform. A performance measures of the suggested CIS-DTC-ADEA approach contains 20.28%, 28.22%, and 29.27% high accuracy, 16.23%, 28.21% and 22.35% higher kappa coefficient and 15.26%, 14.22%, and 22.07% high F-portion when analyzed to the current methods like Comic Unsupervised CD Technique for Heterogeneous RS pictures Based on Copula Mixtures and Cycle-Consistent Adversarial Networks (CUCD-HRSI-CCAN), Deep Learning-Based Classification of the Polar Emotions of “Moe”-Style Cartoon Pictures (CPE-SCP-CNN), High-Precision Matching Algorithm for Multi-Image Segmentation of Micro Animation Videos in Mobile Network Environment (MSMAVMN-HMA) methods respectively.

Keywords: Comic Image Segmentation, Fast Resampled Iterative Filtering, Deep Attention Dilated Residual Convolutional Neural Network, Adaptive Differential Evolution Algorithm.

I. INTRODUCTION

a. Background

In remote sensing (RS), change detection (CD) can be seen being a job for fusion, where the goal is to detect changes in a specific area by combining information from multiple temporal RS pictures taken both prior to and following a particular occasion [1]. Numerous uses for CD exist, including as land management, monitoring urbanization, assessing the effects of natural disasters, and more [2]. Conventional CD methods mostly work on homogenous data, which are RS pictures of the same modality taken with the same kinds of sensors. [3]. The animation sector has evolved into a vast manufacturing chain, offering substantial market potential across gaming, digital entertainment, and related industries [4]. As the cartoon animation market continues to grow, a surplus of cartoon materials accumulates as raw, unprocessed resources. These resources are obtained by several animation studios via a variety of means, and they are then kept as reusable references to aid its artists in producing higher-quality cartoon animation content [5]. Micro animated videos are brief, imaginative, and captivating visual narratives featuring animated characters [6]. They are often crafted by creators drawing from individual preferences, feelings, or opinions, employing humble drawing equipment and noise elements [7]. Comprising multiple brief scenes, each lasting mere seconds, usually lasting between a few mins to many tens of minutes, these films are brief. [8]. Despite their brevity, they possess the power to elicit profound resonance and connection with audiences. Image segmentation stands as a foundational task within image processing and computer vision [9]. Its core objective involves partitioning an image into distinct, non-overlapping regions characterized by shared features like intensity, smoothness, and texture [10]. These features are chosen based on their relevance to the ultimate objective of the segmentation process [11].

b. Challenges

¹School of Comics, Jilin Animation Institute, Changchun, Jilin, 130000, China

*Corresponding author e-mail: 18743293469@163.com

Copyright © JES 2024 on-line : journal.esrgroups.org

Efforts to fully digitize comic books face challenges, particularly in developing systems capable of autonomously extracting their semantic content. The complexity arises from the diverse origins of comic books, encompassing various authors and artists, resulting in a wide array of artistic styles and storytelling methods through images.

This diversity poses limitations on the automation of such extraction processes, necessitating significant human intervention. Although images often exhibit piecewise smooth or flat characteristics, they can also contain non-smooth regions. In practical applications, enforcing smoothness on such images may result in a detrimental averaging of the image content. This process can lead to inaccurate segmentation due to the smoothing out of important details within the image. The alteration map generated from deduction is prone to errors caused by picture conversion, making it challenging to distinguish among altered and unaffected areas. Moreover, in practical CD scenarios, acquiring balancing training information is often impractical before costly. Nonetheless, it's important to acknowledge that training such models can be conducted offline, meaning computational complexity isn't a significant concern in operational scenarios.

c. Literature Review

Several research works presented in the literatures were based on comic image segmentation using deep learning. Some of the reviewed works are outlined below:

Li et al. [12] have suggested the CD using two disparate RS images. Recently, an unsupervised CD method, leveraging the picture conversion approach of CycleGANs within the framework of Expectation-Maximization (EM) algorithm.

Cao et al. [13] have suggested the gaming, digital entertainment, and many other industries have enormous potential for the animation business, which developed into an enormous manufacturing chain. In Oriented Fast and Rotated Binary (ROB) algorithm, the polar emotions conveyed by cartoon materials serve as crucial references for creators, facilitating their access to the necessary imagery.

Su and Y Djenouri [14] have suggested the MSMAVMN-HMA. In mobile network surroundings, the correctness of picture matching procedures can be influenced by issues like bandwidth doubt and channel intrusion, which pose significant challenges to picture feature corresponding.

Lu et al. [15] have suggested the Visual Question Answering (VQA) system entails extracting relevant information from images to accurately answer questions posed about them. This technology finds broad application in areas such as visual assistance, automated security surveillance, and facilitating intelligent interactions between robots and humans.

Zhang et al. [16] have suggested the concentric attention module-based cartoonization style conversion. A widely utilized artistic technique, cartoonization has become deeply ingrained in various aspects of our lives. Cartoonization, a prevalent artistic expression, has seamlessly woven itself into various facets of everyday existence, infiltrating diverse mediums and platforms. Its impact spans entertainment, advertising, education, and social media, enhancing experiences and captivating audiences globally, irrespective of age.

Antonelli et al. [17] have suggested the two-region image segmentation involves dividing an image into two distinct areas of interest: the foreground and the background. To develop a model tailored for smooth images, a novel approach based on cartoon-texture decomposition. This model aims to accurately segment images, even those with noise or oscillatory information such as texture, effectively enhancing segmentation quality across various image types.

Nie et al. [18] have suggested the converting painting images in scenario involving many classes. It conducts deep extracted features in the residual module and divides the decoding and encoding processes of the generator segments into distinct functional units, designed separately. Additionally, incorporating a mixed care module into the encoder and decoder to retain the surface facts of the picture. Furthermore, deep network exclamation was employed to ensure a seamless and ongoing transformation of the painting picture.

d. Research Gap and Motivation

In the domain of CD utilizing RS imagery, recent advancements have introduced unsupervised methods incorporating innovative techniques like CycleGANs within the EM framework. The inaccuracies in derived difference maps undermine the overall efficacy of CD algorithms, necessitating further research to enhance their resilience and applicability. This entails a focus on mitigating complexities arising from disparate RS images and environmental factors. Similarly, within the realm of segmentation of images for wireless network settings' micro-animation videos, existing algorithms encounter substantial hurdles due to bandwidth fluctuations and

channel disturbances. Despite efforts to develop high-precision matching algorithms customized for this context, a crucial research gap remains regarding the scalability and adaptability of these algorithms to varying network conditions and video attributes. Addressing this gap is imperative for advancing mobile-based image segmentation, facilitating more dependable and efficient processing of micro-animation videos across diverse network scenarios.

e. Contribution

The main donations of this manuscript are potted below:

- At first, the data are gathered via the Comic Art Dataset are given as input.
- Fast Resampled Iterative Filtering (FRIF) based pre-processing method for used for noise removal, blur, and binary thresholding.
- The pre-processed data's are fed into the DADRCNN, in order to effectively categorize the manga and classic of the comict data.
- The weights stricture of DADRCNN is optimized using the ADEA
- The efficiency of the suggested example is analyzed with the present methods like ICEI-CUCD-HRSI-CCAN, CPE-SCP-CNN, and MSMAVMN-HMA models respectively.

f. Organization

The remaining manuscripts are arranged as follows: The literature review is reviewed in Part 2, the technique is explained in Part 3, the results are verified in Part 4, and the article is concluded in Part 5.

II. PROPOSED METHODOLOGY

In this section, Comic Image Segmentation and ADEA with Different Times Characteristics (CIS-DTC-ADEA) technique is proposed. Pre-processing begins with the Fast Resampled Iterative Filtering (FRIF), which issued for noise removal, blur, and binary thresholding. The core classification task makes use of the DADRCNN, which is optimized using the ADEA. This approach outperforms existing techniques in terms of Correctness, F-measure, Kappa coefficient, Root Mean Square Error (RMSE), Median mistake, Mean mistake. The block diagram of suggested CIS-DTC-ADEA technique is represented in Fig 1. So, thorough account of all step given as below,

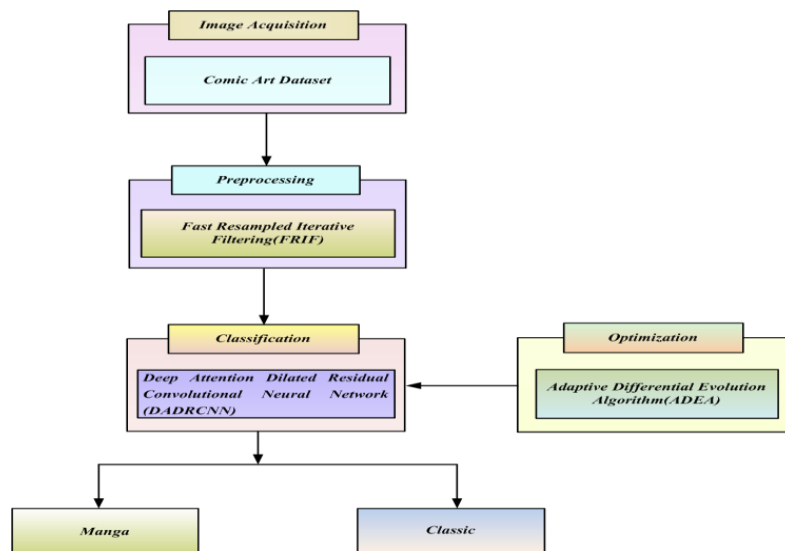


Fig 1: Block diagram of proposed CIS-DTC-ADEA approach

A. Image Acquisition

1) The Comic Art Dataset consists of images categorized into two classes: Manga and Classic [19]. These images are collected from various sources (Google, Bing, and web scraped) and carefully labeled to distinguish between manga-style artwork and classic-style artwork.

2) Classes:

1. Manga: This class includes images that represent artwork typical of manga, a style of Japanese comic books and graphic novels.

2. *Classic: This class includes images that represent classic-style artwork, which may include Western comic book art or traditional comic illustrations.*

B. Pre-Processing Using Fast Resampled Iterative Filtering

In this section, the input images are pre-processed utilizing FRIF [20]. The FRIF is used for noise removal, blur, and binary thresholding. In order to use a discrete version of Robust Interpolated Filtering (RIF), one approach involves separating the shrunk signal's moving a typical basis, as follows

$$g_{n+1}(G(y)) = g_n(G(y)) - \int_R h_n(G(z))K(y-z)dz \tag{1}$$

Notice that $h_n = g_n \circ G$ has a area of $[0, M]$, so it needs to be discretized on a regular grid $y_j = Mi / n$ for $i = 0, \dots, n - 1$. The quadrature rule on a discretization points yields.

$$h_{n+1}(y_j) \approx h_n(y) - \frac{m}{n} \sum_{k \in z} h_n(y_k)k(y_i - y_k) \tag{2}$$

$$K_1 = \frac{m}{n} \left[K(0), K\left(\frac{m}{n}\right), \dots, K\left(s \frac{m}{n}\right), 0, \dots, K\left(s \frac{m}{n}\right), \dots, K\left(\frac{m}{n}\right) \right] \tag{3}$$

Where, $s = n/m$. The moving average is thus given by:

$$h_{n+1} = (I - K)h_n \tag{4}$$

Where, $I - K$ remains a Hermitian and mangle medium, enabling efficient matrix-vector multiplication through FFT. Specifically,

$$h_{n+1} = iDFT((1 - DFT(K_1)) \circ DFT(h_n)) \tag{5}$$

Where " \circ " denotes the Hadamard (or element-wise) produce among courses, and " DFT " and " $iDFT$ " represent the Separate Fourier Alter and its reverse, correspondingly. Additionally, given that

$$DFT(h_{n+1}) = (1 - DFT(K_1)) \circ DFT(h_n) \tag{6}$$

Furthermore, as the discontinuing standard can be assessed on $DFT(h_n)$, we can expedite the process by calculating the DFTs of h_n , K_1 and the $iDFT$ outside the loop. This approach circumvents repetitive calculations of Fourier transforms. After the noise reduction

C. Prediction using Deep Attention Dilated Residual Convolutional Neural Network (DADRCNN)

In this DADRCNN has discussed [21]. This kind of neural network design enhances picture identification and processing tasks by combining many cutting-edge approaches. The DADRCNN is a kind of Convolutional Neural Network (CNN) design that enhances performance in a variety of computer vision applications by integrating dilated convolutions and attention mechanisms. The residual network, a well-liked CNN architecture renowned for its deep residual learning, is the foundation of the DRCNN architecture. Residual learning involves using skip connections can combine a layer's input and output, so resolving the vanishing gradient issue and enabling deeper network training. In adding to the remaining connections, the DRCNN incorporates attention mechanisms. Attention processes allow the network to focus on specific regions or features within the input image that are deemed more important for the task at hand. The network's performance is enhanced and resource allocation made more efficient by this attention technique. The DRM can extract more comprehensive characteristics from the sample picture, the CARM can attention on significant aspects among numerous intricate and variable landslide assessment factors, and the DCU can effectively widen the models' receptive field. Finally, this education builds the DADRCNN construction using the DCU, DRM, and CARM, if a strong network learning model for determining landslide weakness.

The idea of extension is presented by dilated convolution, which builds on the foundation of conventional convolution. As a progressive process, the dilated convolution receptive field of the second layer is closely associated with the amenable field of the coating that came before it. The equation is as follows:

$$R_k = R_{k-1} + (f_k - 1) \times l_k \times \prod_{n=1}^{k-1} S_n \tag{7}$$

In the formula, R_k and R_{k-1} stand in for the convolution kernel's receptive field in the K , and K_1 convolution layers, respectively. Here, f_k is the extent of the difficulty kernel, l_k is the widened factor, and S_n is the difficulty step magnitude.

The ResNet structure is introduced to solve this problem. This structure's primary purpose is to transfer feature data between the upper and lower layers by placing a remaining function mapping layer on top of a shallow network. The deep characteristics of the example pictures characteristics C is removed using dilated difficulty and batch standardization to generate C' , and the residual connection $F(E) + E_0$ is got when the remaining skip connection is made. In below Eqns, the formulas for remaining $F(C)$ and C' has displayed.

$$F(C) = \omega(W_2(\text{Rel}(\omega(W_1C + b_1))) + b_2) \tag{8}$$

$$C' = \omega(W_3E + b_3) \tag{9}$$

Here, W_1, W_2, W_3 represent each dilation convolution layer's parameters, whereas b_1, b_2 , and b_3 represent offsets and ω represent the batch dispensation layer's normalization and the nonlinear start function is known as Rel .

The CARM is introduced taking into account the variable value of several evaluation factors for landslides. The CARM formula is as follows:

$$\beta = Z \oplus Z \otimes \rho((FE(FE(FE(A(Z)))))) \tag{10}$$

Where, $A(\bullet)$ stands for average pooling, FE for fully linked layer, ρ denote a sigmoid purpose, Z for matrices increase, and Y for matrices' addition.

D. Optimizing using Adaptive Differential Evolution Algorithm

The ADEA is advancement in standard DE algorithm. Its distinguishing feature lies in the dynamic adjustment of parameters during optimization [22]. By continuously adapting its strategies according to the problem's characteristics, ADE aims to improve performance and convergence speed. Throughout the optimization process, ADE fine-tunes parameters like mutation strategies, crossover probabilities, and scaling factors. This adaptability enables the algorithm to achieve equilibrium between discovery and use, thereby enhancing its capability to discover optimal solutions in intricate and evolving optimization landscapes. In essence, the ADEA optimizes its parameters, tailoring them to the specific demands of the problem at hand. This flexibility enhances its efficacy and efficiency in navigating towards optimal solutions.

Step 1: Initialization

Reset the input limits, here the input parameter are the weight parameter search agents is shown in Eqn (11)

$$y_i d = LB_d + R.(UB_d - LB_d) \tag{11}$$

Where, $y_i d$ denote the d^{th} dimension in the search space for a decision variable, i ranges, let R be a random amount selected consistently from the interval [0, 1]. Then LB_d and UB_d represent the inferior and upper bounds, respectively, for the d^{th} choice variable.

Step 2: Random Generation

After initialization, weight limits are formed arbitrarily generated. The standards of best fitness are selected contingent explicit hyper parameter situation.

Step 3: Fitness Calculation

Fitness is dependent on the objective purpose. The definition of the health function is

$$\text{Fitness Function} = \text{optimizing}(\rho \text{ and } \omega) \tag{12}$$

The random response is the outcome, which is derived from the initialized assessments. The fitness function evaluation makes advantage of the weight parameter optimization effects. It is stated in Equation (12).

Step 4: Mutation for Optimizing ρ

The mutation operation plays a crucial role. DE employs the alteration operation in each group g to generate a alteration vector $V_{l,g+1}$ for every separate $X_{r1,g}$. Various mutation strategies are normally engaged in DE.

$$\omega = DE / rand / 1 : V_{l,g+1} = X_{r1,g} + f * (y_{r1,g} - y_{r3,g}) \tag{13}$$

$$DE / rand / 2 : V_{I,g+1} = X_{r1,g} + f * (y_{r1,g} - y_{r3,g}) + f * (y_{r4,g} - y_{r5,g}) \quad (14)$$

Where, ω represent the batch processing layer's normalization the indices $r1, r2, r3, r4, ,$ and $r5$ are separate from index $I(r1, r2, r3, r4, r5)$ and are selected within the interval $[1, NP]$. An essential control parameter in DE is the climbing factor $f \in [0, 2]$, which regulates a amplification greatness of the vectors that differ.

Step 5: Crossover for Optimizing ω

After the mutation operation, DE frequently employs creating a new crossover vector using the binomial crossover procedure $U_{I,g+1}$ by uniting the fundamentals of the target course $y_{I,g}$, and the alteration course $V_{I,g+1}$. This procedure enhances a variety of populace as a whole; Eqn (15) delineates the crossing mechanism. DE often creates a new crossover vector using the binomial crossover operation after the mutation procedure. $U_{I,g+1}$ by putting the board vector's components back together $y_{I,g}$ and a alteration vector $V_{I,g+1}$. This growths the variety of the whole populace and the Eqn (15) signifies the journey instrument.

$$\rho = U_{I,g+1}^J = \begin{cases} V_{I,g+1}^J, & \text{if } rand(J) < CR \text{ or } J = rnbr(I) \\ y_{I,g}^J, & \text{if } rand(J) > CR \text{ or } J \neq rnbr(I) \end{cases} \quad (15)$$

Where $J = 1, 2 \dots D, rand(J), rand(J) \in [0, 1]$ represents a consistently distributed chance amount. $CR \in [0, 1]$ is a user-specified control limit denoting the crossover ratio and ρ denote a sigmoid function,. $rnbr(I)$ is an number randomly designated from the series $[0, D]$, ensuring that the crossover vector $U_{I,g+1}^J$ may inherit at least one stricture from the alteration vector $V_{I,g+1}^J$. To determine which vector among the crossover vector $U_{I,g+1}$ and the target vector $y_{I,g}^J$ will survive to generate offspring, DE services a greedy approach by likening the suitability values of the two vectors. The vector with the inferior fitness value will spread to the next group if the impartial purpose is aimed at minimization.

Step 6: Update the Best Solution

After acquiring both the present population and the changed population, the algorithm proceeds to perform uniform crossover between the two populations to generate a mixed population. This operation aims to enhance the probability of obtaining a superior global optimal solution. Utilizing the crossover likelihood cr , the procedure selects nodes from the separate Y_I of the present generation or the altered separate to create the new discrete. The rudiments within a specific crossover individual are generated following the rules outlined in Eqn (16).

$$C_{IJ} = \begin{cases} y_{IJ} \text{ or unique}(DDS(nodelist, I)), & \text{if } rand(0,1) > cr \\ n_{IJ} \text{ or unique}(DDS(nodelist, I)), & \text{if } rand(0,1) \leq cr \end{cases} \quad (16)$$

Where, c_{IJ} , y_{IJ} and n_{IJ} represent a single node of the border individual C_I the present individual Y_I , and the changed individual N_I , respectively.







Step 7: Termination

The process ends when the solution is deemed optimal; otherwise, it iterates back to Step 3 for fitness calculation and proceeds through the subsequent steps until the optimal solution is attained.

III. RESULT AND DISCUSSION

It discussed outcomes of the study conducted by the suggested approach. Next, a suggested method is simulated under the specified performance criteria using the Python working platform. The found outcome of the anticipated CIS-DTC-ADEA approach is examined with current systems like CUCD-HRSI-CCAN, CPE-SCP-CNN, and MSMAVMN-HMA respectively. The output of the proposed CIS-DTC-ADEA process is shown in Table 1.

Table 1: The output of the proposed CIS-DTC-ADEA method

Input Image	Pre-Processed Image	Segmented Image	Classification
			Manga
			Classic

A. Performance measures

In order to choose the optimal classifier, this is an important task. Performance indicators including accuracy, F-measure, kappa coefficient, RMSE, median error, and mean error are analyzed in order to measure the presentation. The misperception matrix is considered in order to scale the performance indicators. To scale the misperception matrix, the True Negative (TN), True Positive (TP), False Negative (FN) and False Positive (FP) ethics are needed.

1) Accuracy

The capability to measure precise value is called as accuracy. A statistic called accuracy may be utilized to characterize the model's presentation in all classes. It is measured by a next expressed Eqn (17)

$$Accuracy = \frac{(TP + TN)}{(TP + FP + TN + FN)} \tag{17}$$

2). Kappa Coefficient

$$KC = \frac{2(TP \times TN - FN \times FP)}{(TP + FP) \times (FP + TN) \times (TP + FN) \times (FN + TN)} \tag{18}$$

3) F-measure

F-amount is a metric utilized to analyze the presentation of proposed CIS-DTC-ADEA technique. It is computed in Eqn (19),

$$Fm = \frac{2TP}{2TP + FP + FN} \tag{19}$$

4) RMSE

$$RMSE = \sqrt{\frac{\sum [(y_i - \bar{Y}_i)^2 + (z_i - \bar{Z}_i)^2]}{n}} \tag{20}$$

In the context of a micro-animation video, where (y_i, z_i) represent points in the original image and (Y_i, Z_i) represent corresponding points in the target image,

5) Median Measure

$$\tau = \sqrt{\frac{\sum [(y_i - \bar{Y}_i)^2 + (Y_i - \bar{Y}_i)^2 + (z_i - \bar{Z}_i)^2 + (Z_i - \bar{Z}_i)^2]}{n}} \tag{21}$$

Where, τ is represent the median error, the average of the coordinates for each pair of points (y_i, z_i) and (Y_i, Z_i) is calculated, denoted as the average of (y_i, z_i) and (Y_i, Z_i) , for $i = 1, 2, \dots, n$.

B. Performance Analysis

Fig 2 to 7 shows the simulation outcomes of CIS-DTC-ADEA. Then the outcomes are analyzed with existing CUCD-HRSI-CCAN, CPE-SCP-CNN, and MSMAMVN-HMA methods.

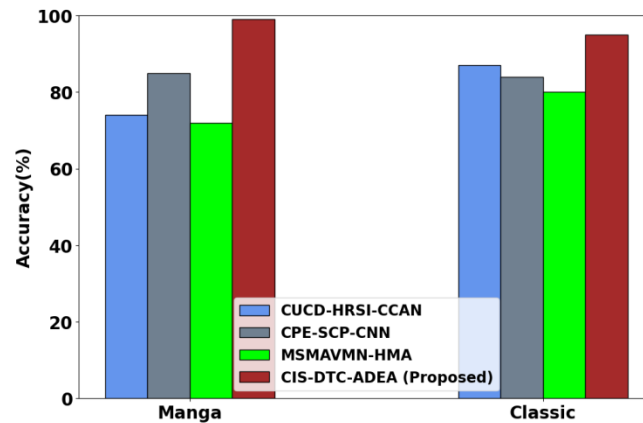


Fig 2: Performance analysis of accuracy with proposed and existing approaches

Fig 2 depicts the presentation of correctness with planned and current approaches. Here proposed CIS-DTC-ADEA technique results in accuracy that are 20.28%, 28.22%, and 29.27% higher for the classification of manga, 26.29%, 17.31%, and 17.26% higher for the classification of classic when evaluated to the existing CUCD-HRSI-CCAN, CPE-SCP-CNN, and MSMAMVN-HMA models correspondingly.

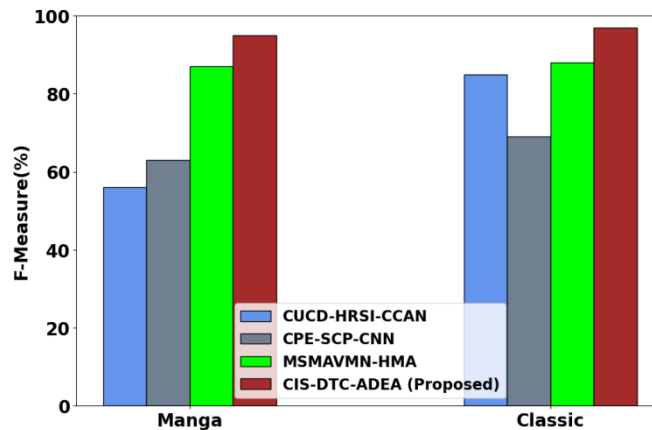


Fig 3: Performance analysis of F-measure value with proposed and existing method

Fig 3 shows the analysis of F-measure value with planned and present method. The performance of the proposed CIS-DTC-ADEA technique results in F-measure that are 22.56%, 21.76%, 33.97%, higher for the organization of manga, 21.46%, 33.58%, 23.54% higher for the classification of classic when estimated to the present CUCD-HRSI-CCAN, CPE-SCP-CNN, and MSMAMVN-HMA models individually.

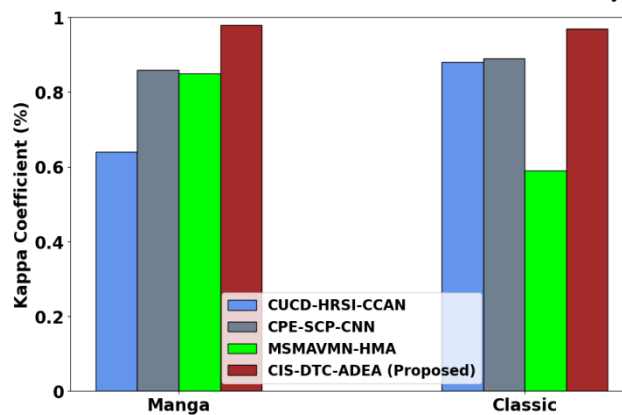


Fig 4: Performance analysis of kappa coefficient with proposed and existing method

Fig 4 shows the performance examination of kappa coefficient with planned and existing method. The performance of the proposed CIS-DTC-ADEA technique results in kappa coefficient that are 28.26%, 15.22%, and 22.27% higher for classification of manga, 16.23%, 28.21% and 22.35%, higher for classification of classic

when evaluated to the existing approaches such as CUCD-HRSI-CCAN, CPE-SCP-CNN, and MSMVMN-HMA correspondingly.

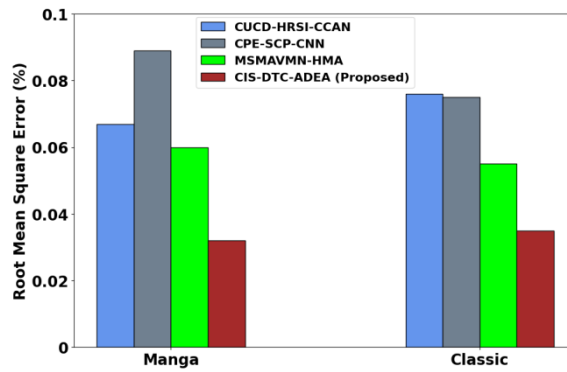


Fig 5: Performance analysis of RMSE with proposed and existing method

Fig 5 shows the analysis of RMSE with planned and present method. The performance of the proposed CIS-DTC-ADEA technique results in RMSE that are 11.20%, 13.25%, and 32.08% lower for the classification of manga, 31.14%, 20.07 %, and 17. 71% lower for the classification of classicwhen evaluated to the existing methods such as CUCD-HRSI-CCAN, CPE-SCP-CNN, and MSMVMN-HMA respectively.

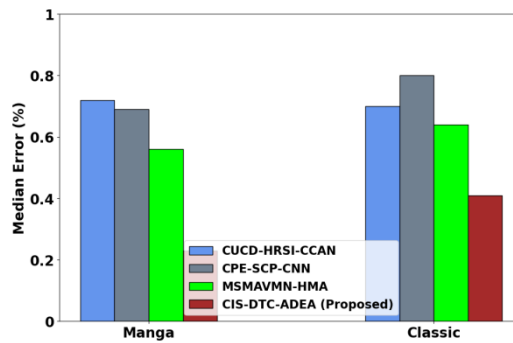


Fig 6: Performance analysis of median error with proposed and existing method

Fig 6 shows the performance examination of median error with planned and present method. The performance of the proposed CIS-DTC-ADEA technique results in median error that are 23.21%, 13.22%, and 12.22% lower for the classification of manga, 35.14%, 10.56 %, and 16. 25% lower for the classification of classicwhen evaluated to the existing methods such as CUCD-HRSI-CCAN, CPE-SCP-CNN, and MSMVMN-HMA respectively.

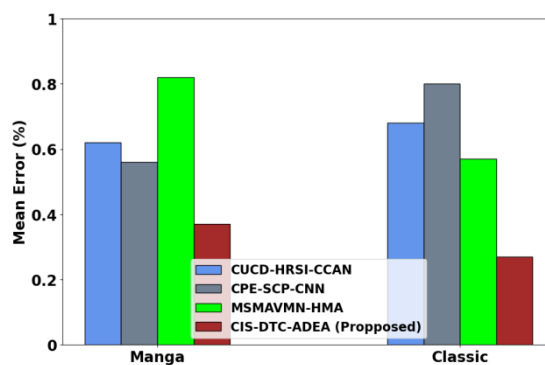


Fig 7: Performance analysis of mean error with proposed and existing method

Fig 7 shows the performance examination of mean mistake with planned and current method. The performance of the proposed CIS-DTC-ADEA technique results in mean error that are13.20%, 11.22%, and 22.07% lower for the classification of manga, 25.14%, 20.07 %, and 16. 75% lower for the classification of classic when evaluated to the existing methods such as CUCD-HRSI-CCAN, CPE-SCP-CNN, and MSMVMN-HMA respectively

C. Discussion

This manuscript proposes Comic Image Segmentation ADEA with Different Times Characteristics. The proposed CIS-DTC-ADEA approach is implemented in python working platform. Across all metrics and both classification categories (manga and classic), the CIS-DTC-ADEA technique consistently outperforms existing methods. For instance, in terms of accuracy, the proposed technique yields significantly higher accuracy rates compared to existing models, with improvements ranging from around 20% to nearly 30%. F-measure analysis, the CIS-DTC-ADEA technique demonstrates substantial performance gains, with improvements ranging from approximately 21% to almost 34% for manga classification, and from about 21% to over 33% for classic classification, when compared to existing methods. Moreover, the kappa coefficient analysis further confirms the superiority of the proposed technique, showing notable improvements ranging from around 15% to over 28% for manga classification, and from approximately 16% to more than 28% for classic classification, relative to existing approaches. The evaluation of RMSE reveals significant reductions in error rates achieved by the CIS-DTC-ADEA technique, with decreases ranging from about 11% to over 32% for manga classification, and from around 17% to over 31% for classic classification, in comparison to existing methods. Furthermore, both median error and mean error analyses demonstrate substantial decreases in error metrics, indicating the superior performance of the proposed technique across different evaluation perspectives. In summary, the CIS-DTC-ADEA technique consistently exhibits superior performance compared to existing methods across various evaluation metrics and classification categories. These findings suggest the effectiveness and efficiency of the proposed approach in accurately classifying manga and classic categories, which could have significant implications for applications requiring precise classification algorithms.

IV. CONCLUSION

In this section, CIS-DTC-ADEA were successfully implemented in python. The proposed method CIS-DTC-ADEA is used to classifying images such as manga and classic. Evaluating the performance of approach, the results highlight distinct improvements and achieving 29.2%, 26.5%, and 31.4% Accuracy, 16.5%, 18.8%, 11.4% kappa coefficient and 24.65%, 11.66%, 23.97% F-measure are compared with existing methods like CUCD-HRSI-CCAN, CPE-SCP-CNN, and MSMAMVN-HMA respectively. Future work in the field of comic image segmentation could involve integrating advanced machine learning techniques with domain-specific knowledge to enhance segmentation accuracy and efficiency. Additionally, exploring novel approaches for addressing challenging aspects of comic images, such as varying art styles, panel layouts, and text fonts, could further improve segmentation performance. Moreover, developing methods for automatic parameter tuning and adaptation within segmentation algorithms, especially in conjunction with deep learning models like DeepLabv3+, could lead to more robust and versatile segmentation solutions for diverse comic image datasets. Furthermore, delving into the potential applications of comic image segmentation beyond content retrieval and production, such as in interactive storytelling, artistic expression, and educational tools, offers promising avenues for future research and development.

Acknowledgements

This article is the research result of the Social Science Research Project of the Department of Education of Jilin Province, China, "Research on Historical Memory and National Unity Education in Revolutionary Comics during the Anti-Japanese War" (No.: JJKH20241470SK).

REFERENCE

- [1] Wang, L., & Ma, C. (2022). Research on Character Action Recognition of Digital Comics. *Procedia Computer Science*, 208, 286-292.
- [2] Chen, H., Liu, Y., Zhang, P., Kang, J., Li, Z., Cheng, W., & Gui, Z. (2024). Low-Dose CT Denoising Algorithm Based on Image Cartoon Texture Decomposition. *Circuits, Systems, and Signal Processing*, 1-29.
- [3] Xin, H., & Jin, X. (2024). Text feature-based copyright recognition method for comics. *Engineering Applications of Artificial Intelligence*, 132, 107925.
- [4] Zhang, B., Zhao, H., Si, M., Cui, W., Zhou, Y., Fu, S., & Wang, H. (2024). RC-Net: A region-level context network for hyperreflective dots segmentation in retinal OCT images. *Optics and Lasers in Engineering*, 172, 107872.
- [5] Long, J., & Zhang, C. (2024). Image smoothing combining edge-consistency with region-piecewise flattening. *Computers & Graphics*, 118, 90-101.
- [6] Sawada, T., & Katsurai, M. (2024). Illustrated character face super-deformation via unsupervised image-to-image translation. *Multimedia Systems*, 30(2), 63.

- [7] Dutta, A., Biswas, S., & Das, A. K. (2024). EmoComicNet: A multi-task model for comic emotion recognition. *Pattern Recognition*, 150, 110261.
- [8] Christopher, A. M. (2024). "The boy in the cupboard": children in Indian comics and their subversion of heteronormative interpellation. *Journal of Graphic Novels and Comics*, 1-18.
- [9] Wu, X., Zhang, K., Hu, Y., He, X., & Gao, X. (2024). Multi-scale non-local attention network for image super-resolution. *Signal Processing*, 218, 109362.
- [10] Zhao, W., Zhu, J., Li, P., Huang, J., & Tang, J. (2024). Attention mechanism-based generative adversarial networks for image cartoonization. *The Visual Computer*, 1-14.
- [11] Yang, Y., Xu, Z., & Zhang, Y. (2024). Screen content image quality measurement based on multiple features. *Multimedia Tools and Applications*, 1-28.
- [12] Li, C., Li, G., Wang, Z., Wang, X., & Varshney, P. K. (2024). COMIC: An unsupervised change detection method for heterogeneous remote sensing images based on copula mixtures and Cycle-Consistent Adversarial Networks. *Information Fusion*, 106, 102240.
- [13] Cao, Q., Zhang, W., & Zhu, Y. (2020). Deep learning-based classification of the polar emotions of "moe"-style cartoon pictures. *Tsinghua Science and Technology*, 26(3), 275-286.
- [14] Su, Y., & Djenouri, Y. (2023). High-precision matching algorithm for multi-image segmentation of micro animation videos in mobile network environment. *Mobile Networks and Applications*, 1-11.
- [15] Lu, S., Ding, Y., Liu, M., Yin, Z., Yin, L., & Zheng, W. (2023). Multiscale feature extraction and fusion of image and text in VQA. *International Journal of Computational Intelligence Systems*, 16(1), 54.
- [16] Zhang, F., Zhao, H., Li, Y., Wu, Y., & Sun, X. (2023). CBA-GAN: Cartoonization style transformation based on the convolutional attention module. *Computers and Electrical Engineering*, 106, 108575.
- [17] Antonelli, L., De Simone, V., & Viola, M. (2023). Cartoon-texture evolution for two-region image segmentation. *Computational Optimization and Applications*, 84(1), 5-26.
- [18] Nie, X., & Pu, J. (2023). Mixed Attention Mechanism Generative Adversarial Network Painting Image Conversion Algorithm Based on Multi-Class Scenes. *IEEE Access*, 11, 123242-123252.
- [19] <https://www.kaggle.com/datasets/kaustubhrastogi17/manga-and-classic-comic-arts>
- [20] Barbarino, G., & Cicone, A. (2024). Stabilization and variations to the adaptive local iterative filtering algorithm: The fast resampled iterative filtering method. *Numerische Mathematik*, 1-39.
- [21] Ma, Y., Xu, S., Jiang, T., Wang, Z., Wang, Y., Liu, M., ... & Ma, X. (2023). Learning a Deep Attention Dilated Residual Convolutional Neural Network for Landslide Susceptibility Mapping in Hanzhong City, Shaanxi Province, China. *Remote Sensing*, 15(13), 3296.
- [22] Tang, J., Du, Q., Qu, J., Li, Y., & Han, L. (2024). An adaptive differential evolution algorithm driven by multiple probabilistic mutation strategies for influence maximization in social networks.